ISSN 1063-7834, Physics of the Solid State, 2007, Vol. 49, No. 4, pp. 734–738. © Pleiades Publishing, Ltd., 2007.
Original Russian Text © S.V. Komogortsev, R.S. Iskhakov, A.D. Balaev, A.G. Kudashov, A.V. Okotrub, S.I. Smirnov, 2007, published in Fizika Tverdogo Tela, 2007, Vol. 49, No. 4, pp. 700–703.

MAGNETISM AND FERROELECTRICITY

Magnetic Properties of Fe_3C Ferromagnetic Nanoparticles Encapsulated in Carbon Nanotubes

S. V. Komogortsev[a], R. S. Iskhakov[a], A. D. Balaev[a], A. G. Kudashov[b], A. V. Okotrub[b], and S. I. Smirnov[c]

[a] *Kirensky Institute of Physics, Siberian Division, Russian Academy of Sciences, Akademgorodok, Krasnoyarsk, 660036 Russia*
e-mail: komogor@iph.krasn.ru
[b] *Nikolaev Institute of Inorganic Chemistry, Siberian Division, Russian Academy of Sciences, ul. Akademika Lavrent'eva 3, Novosibirsk, 660090 Russia*
[c] *Krasnoyarsk State Pedagogical University, ul. Lebedevoy 79, Krasnoyarsk, 660017 Russia*

Received July 25, 2006

Abstract—The low-temperature dependences of magnetic characteristics (namely, the coercive force H_c, the remanent magnetization M_r, local magnetic anisotropy fields H_a, and the saturation magnetization M_s) determined from the irreversible and reversible parts of the magnetization curves for Fe_3C ferromagnetic nanoparticles encapsulated in carbon nanotubes are investigated experimentally. The behavior of the temperature dependences of the coercive force $H_c(T)$ and the remanent magnetization $M_r(T)$ indicates a single-domain structure of the particles under study and makes it possible to estimate their blocking temperature $T_B = 420$–450 K. It is found that the saturation magnetization M_s and the local magnetic anisotropy field H_a vary with temperature as $\sim T^{5/2}$.

PACS numbers: 75.75.+a, 61.46.Df, 65.80.+n, 75.30.-m, 75.60.Nt

DOI: 10.1134/S1063783407040233

1. INTRODUCTION

The properties of nanoparticles differ considerably from those of particles several fractions of a micrometer in size or larger. Let us consider the possible reasons for these differences [1–5].

(1) Nanoparticles are intermediate objects between bulk systems and atoms, and, therefore, as the number of atoms in a nanoparticle increases, the properties of these objects change from those characteristic of a single atom to the properties of a bulk body (quantum-chemical description).

(2) The fraction of surface atoms in a nanoparticle is comparable to that of bulk atoms; consequently, the surface contribution gives rise to new properties and even novel, unusual structural states.

(3)The size of nanoparticles becomes comparable to the characteristic scale of variation in the physical properties of a material (the size effect).

(4) Since the small size of nanoparticles makes collective excitations with wavelengths in excess of the nanoparticle sizes impossible, the thermodynamic properties of the nanoparticles change significantly (the so-called finite size effect) [5].

A comprehensive theoretical description of the properties of nanoparticles, their ensembles, and nanomaterials is still lacking, and relevant experimental data are just now being accumulated.

Based on the magnetic properties of an ensemble of small particles, magnetic nanoparticles can be grouped in two classes, namely, superparamagnetic particles (usually with sizes ranging from 1 to 10 nm) and ferromagnetic particles (10–50 nm). The magnetic properties of systems of superparamagnetic particles are explained in terms of the theory of superparamagnetic relaxation, which is based on the assumption that the material inside each such particle is ferromagnetically ordered. Obviously, a more thorough experimental investigation of the thermodynamic properties of nanoparticles near the ground state can be carried out using ferromagnetic nanoparticles.

Experimental studies of magnetic nanoparticles of Fe, Co, and Ni, as well as alloys based on these metals, are complicated by the fact that, under standard atmospheric conditions, nanoparticles are coated with an oxide film comparable in thickness to the size of the particle itself. To prevent the formation of oxide layers, nanoparticles are prepared in special matrices or encapsulated in a shell of a material precluding oxidation [3, 4, 6]. However, this technological problem is far from simple. For nanoparticles, there is virtually no inert medium because of their extremely high chemical activity [4]. The best solution to this problem is offered by the use of nanoparticles of Fe, Co, and Ni, as well as their alloys, which are employed as catalysts for the growth of carbon nanotubes and, consequently, are encapsulated in the nanotubes. Owing to the chemically

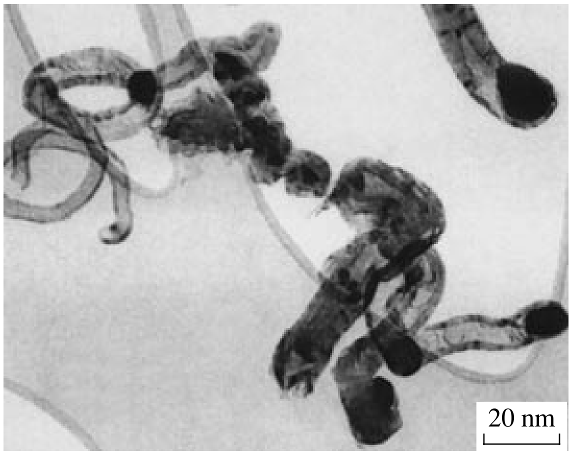

Fig. 1. TEM image of the carbon nanotubes filled with iron nanoparticles.

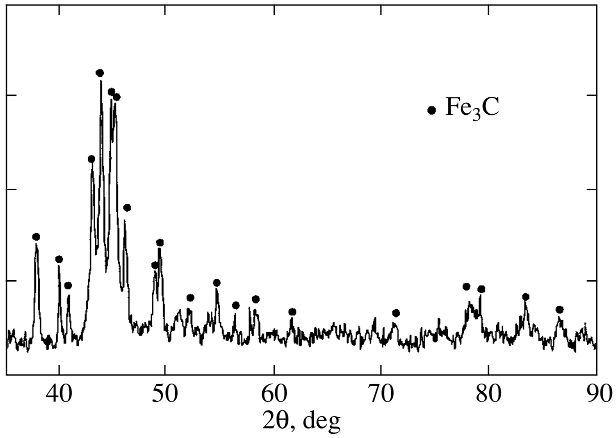

Fig. 2. X-ray diffraction pattern of the Fe–C nanoparticles in carbon nanotubes.

closed and extremely strong bonds of carbon forming nanotube walls, a carbon nanotube serves as the most inert capsule for nanoparticles of Fe, Co, and Ni, as well as for their alloys [4, 6–9].

The purpose of this work was to investigate the low-temperature dependences of the magnetic properties of Fe_3C ferromagnetic nanoparticles encapsulated in carbon nanotubes, which were derived from the irreversible (coercive force H_c, remanent magnetization M_r) and reversible (local magnetic anisotropy fields H_a, saturation magnetization M_s) parts of the magnetization curves.

2. SAMPLE PREPARATION AND EXPERIMENTAL TECHNIQUE

We studied Fe–C nanoparticles encapsulated in carbon nanotubes and synthesized through thermal decomposition of the $C_6H_4(COO)_2Fe$ maleate [9].

The samples thus prepared were studied with a JEOL 100 C transmission electron microscope (TEM) and a DRON-SEIFERT-RM4 diffractometer. Static magnetic measurements were performed on a computerized vibrating-sample magnetometer in magnetic fields of up to 8 kOe at temperatures ranging from 77 to 300 K. A holder with an empty capsule intended to contain a powder sample was measured separately, and its contribution to the total signal (~1%) was subtracted. The magnetization curves were obtained for temperatures of 77, 90, and 100 K and, thereafter, in 10-K steps up to 320 K.

Figure 1 displays the TEM images of nanotubes. We readily see that the nanotubes are partially filled with iron (the dark regions in the images correspond to Fe particles, and the semitransparent regions, to the graphite walls). The measured values of the saturation magnetization permit us to estimate the weight fraction of Fe in these nanocomposites. It was found that the weight fraction of Fe is ~8%. The inner diameter of these nanotubes is ~100 Å. X-ray diffraction analysis showed that the nanoparticles inside the nanotubes are particles of iron carbide Fe_3C. Indeed, all the reflections observed in the x-ray diffraction pattern (Fig. 2) can be identified with those from the system of crystallographic planes of cementite Fe_3C.

3. RESULTS AND DISCUSSION

Figure 3 depicts 25 magnetization curves for the nanoparticles under study. These curves were obtained by reducing the external field from 8 kOe to negative values corresponding to the coercive force H_c. The insets to Fig. 3 show the magnetization curves measured at temperatures of 77 and 320 K. It can be seen

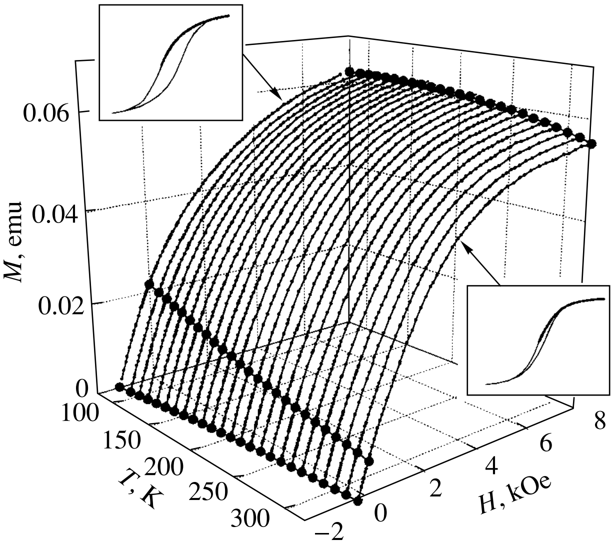

Fig. 3. Temperature dependence of the magnetization curves for Fe_3C nanoparticles in carbon nanotubes.

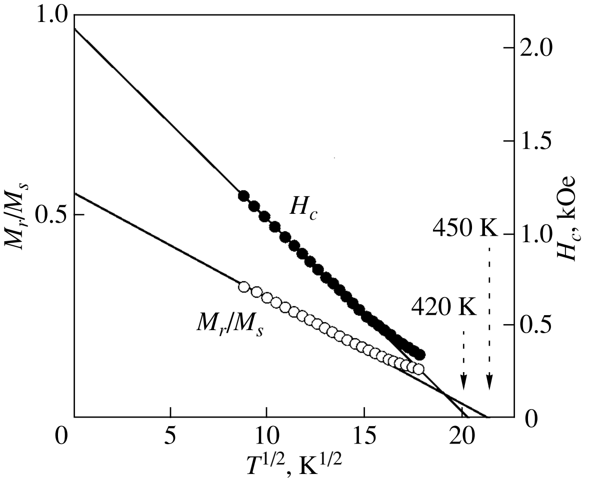

Fig. 4. Temperature dependences of the coercive force H_c and the remanent magnetization M_r/M_s for Fe_3C nanoparticles in carbon nanotubes.

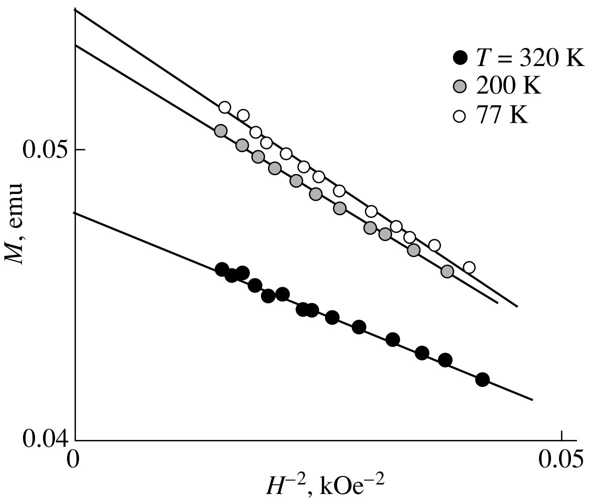

Fig. 5. Behavior of the magnetization approaching saturation for Fe_3C nanoparticles in carbon nanotubes.

that the curves $M(H)$ obtained in the range from –8 to 8 kOe are symmetric with respect to the origin and contain a reversible part, which is characterized by a unique dependence of the magnetization M on the magnetic field H, and an irreversible part, namely, a hysteresis loop. The sections of the three-dimensional diagram plotted in the (M, H, T) coordinates in Fig. 3 make it easier to follow the temperature dependences of the corresponding magnetic characteristics. Actually, the $(M = 0, H, T)$ section describes the temperature dependence of the coercive force $H_c(T)$, the $(M, H = 0, T)$ section shows the temperature dependence of the remanent magnetization $M_r(T)$, and the $(M, H = 8$ kOe$, T)$ section represents the temperature dependence of the magnetization in a magnetic field of 8 kOe. As can be seen, the magnetic characteristics decrease with increasing temperature.

The experimental data presented in Fig. 4 show that the coercive force decreases with increasing temperature according to the power law $H_c \sim T^{1/2}$. This dependence is characteristic of single-domain noninteracting nanoparticles at temperatures below the blocking temperature (T_B) [10]:

$$H_c(T) = H_c(0)(1-(T/T_B)^{1/2}). \qquad (1)$$

Therefore, the dependence $H_c(T)$ plotted in the $T^{1/2}$–H_c coordinates makes it possible to estimate the blocking temperature by extrapolating the straight-line portion from the low-temperature range to the point corresponding to $H_c = 0$ on the ordinate axis. From expression (1), the blocking temperature was estimated as $T_B = 420$ K. It turned out that the dependence $M_r(T)$ plotted in Fig. 4 can also be described by the relationship $M_r \sim T^{1/2}$. Extrapolating the straight-line portion of this dependence from the low-temperature range to the point $M_r = 0$ on the ordinate axis, we obtain the blocking temperature $T_B = 450$ K. Extrapolating the same straight-line portion of the dependence $M_r(T^{1/2})$ to $T = 0$ on the abscissa axis, we find $M_r/M_s \approx 0.5$, which is close to the remanent magnetization in the Stoner–Wohlfahrt model.

It is worth noting that all numerical estimates of the blocking temperature T_B do not exceed the Curie temperature for Fe_3C (483 K). Therefore, the dependences $H_c(T)$ and $M_r(T)$ in this case can be adequately described in terms of thermal relaxation theory. Note also that these estimates of the blocking temperature are substantially higher than the temperatures at which the magnetization curves were measured. This suggests that the superparamagnetic contribution to the experimental dependence $M(T, H)$ is insignificant.

Figure 5 presents the high-field reversible parts of the magnetization curves measured for the studied nanoparticles at $T = 77$, 200, and 320 K and plotted in the H^2–M coordinates. The straight-line portions in these dependences (Fig. 5) indicate the functional dependence $M \sim H^2$. This functional dependence was observed in all the measured magnetization curves (for clarity, only three isotherms are depicted in Fig. 5). Therefore, the magnetization curves of nanoparticles containing Fe that are encapsulated inside carbon nanotubes are fitted by the Akulov law:

$$\frac{M(H)}{M_s} = 1-\frac{1}{15}\left(\frac{H_a}{H}\right)^2, \qquad (2)$$

where $H_a = 2K/M_s$ is the local magnetic anisotropy field in a nanoparticle and M_s is the saturation magnetization of this particle. It is known that the Akulov law describes the magnetization as it approaches saturation in polycrystals with large grains not coupled by exchange interaction [11]. This law is also valid when describing the magnetization of single-domain noninteracting ferromagnetic particles. The magnetization curve for a system of exchange-coupled nanoparticles is described by other power relationships [12]. Thus, the dependence $M \sim H^2$ revealed in the experiment suggests that the nanoparticles under investigation have a single-domain structure and are not involved in exchange interaction.

Figure 6 presents the temperature dependences of the main parameters derived from expression (2), which characterize the magnetization curve. It was found that the saturation magnetization M_s and the local magnetic anisotropy fields H_a decrease with increasing temperature according to the same power law:

$$M_s(T) = M_s(0)(1 - C_M T^{5/2}), \tag{3}$$

$$H_a(T) = H_a(0)(1 - C_A T^{5/2}), \tag{4}$$

where $C_M = 1.1 \times 10^{-7}$ K$^{-5/2}$ and $C_A = 1.4 \times 10^{-7}$ K$^{-5/2}$.

It is known that, in the general case, deviations of the magnetization from complete saturation are determined by thermal spin waves and spatial orientation fluctuations of the unit vector of the easy magnetization axis $l(r)$. However, the experimental temperature dependence of the saturation magnetization determined from the asymptotics $H \longrightarrow \infty$ is governed only by the contribution from thermal spin waves. For this reason, primary attention is drawn to the deviation of the above dependence of the saturation magnetization of nanoparticles (Fig. 6) from the well-known Bloch law $T^{3/2}$. We believe that the observed deviation of the dependence $M_s(T)$ from the law $T^{3/2}$ for Fe_3C nanoparticles is caused by a change in the spectral characteristics of thermal spin excitations in small particles (the so-called finite size effect) [5]. In particular, Hendriksen et al. [5] showed that the spectral properties of spin waves in nanoparticles differ substantially from those observed in a bulk material; as a result, such a thermodynamic property as the temperature dependence of the spontaneous magnetization shows a different behavior. It turned out that, in our case, the temperature dependence of the spontaneous magnetization should follow the law $M_s \sim T^{\alpha}$, where $3/2 < \alpha < 3$. We note also that the temperature gradient $(M_s(77\text{ K}) - M_s(300\text{ K}))/M_s(77\text{ K})$ (which is proportional to the rate of increase in the number of thermal magnons) for bulk samples of cementite is 13% [13]. A similar temperature gradient was obtained in our experiment.

The temperature dependence of the local magnetic anisotropy field $H_a(T)$ is similar to the dependence $M_s(T)$. The temperature gradients of $H_a(T)$ and $M_s(T)$ are likewise approximately equal. Thus, the data presented in Fig. 6 also indicate that $H_a(T) \sim M_s(T)$. In the general case, the local magnetic anisotropy field in nanoparticles can be governed by several contributions, more specifically, the contribution from the crystallographic magnetic anisotropy, the contribution from the anisotropy induced by internal stresses, and the contribution from the anisotropy in the particle shape. The first two of the above contributions to the local magnetic anisotropy field are proportional to the saturation magnetization squared [14]. As regards the local magnetic anisotropy associated with the shape anisotropy, it depends linearly on the saturation magnetization M_s [15]. Hence, the local magnetic anisotropy of the nanoparticles studied here should primarily be related to the shape anisotropy of these particles.

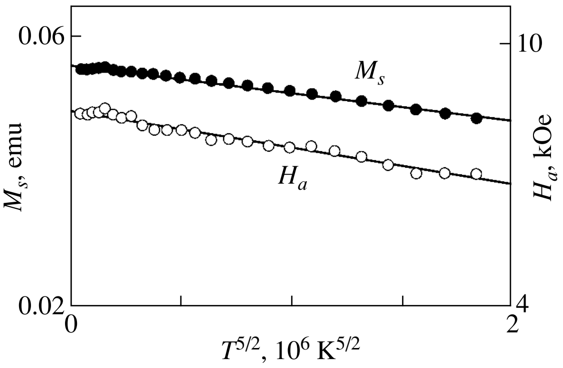

Fig. 6. Temperature dependences of the saturation magnetization M_s and the local magnetic anisotropy field H_a.

4. CONCLUSIONS

Thus, Fe_3C ferromagnetic nanoparticles encapsulated in carbon nanotubes were characterized by the quantities H_c, M_r, H_a, and M_s. It was found that the temperature dependences of the coercive force H_c and the remanent magnetization M_r of these nanoparticles can be adequately described in terms of thermal relaxation theory. Moreover, it was established that the saturation magnetization M_s varies with temperature as $M_s \sim T^{5/2}$, which is inconsistent with the dependence predicted by the standard theory of spin waves. It was shown that the main contribution to the local magnetic anisotropy field H_a of Fe_3C nanoparticles encapsulated in carbon nanotubes comes from the shape anisotropy of these particles.

ACKNOWLEDGMENTS

This study was supported by the program “Development of the Scientific Potential of the Higher School (2006–2008)” (project no. RNP.2.1.1.7376) and the Russian Foundation for Basic Research (project no. 06-03-32802-a).

REFERENCES

1. Yu. I. Petrov, *Physics of Small Particles* (Nauka, Moscow, 1982) [in Russian].

2. S. A. Nepiĭko, *Physical Properties of Small Particles* (Naukova Dumka, Kiev, 1985) [in Russian].
3. S. P. Gubin and Yu. A. Koksharov, Neorg. Mater. **38** (11), 1287 (2002) [Inorg. Mater. **38** (11), 1085 (2002)].
4. A. L. Buchachenko, Usp. Khim. **72** (5), 419 (2003) [Russ. Chem. Rev. **72** (5), 375 (2003)].
5. P. V. Hendriksen, S. Linderoth, and P. A. Lindgård, Phys. Rev. B: Condens. Matter **48**, 7259 (1993).
6. D. Zhang, K. J. Klabunde, C. M. Sorensen, and G. C. Hadjipanayis, Phys. Rev. B: Condens. Matter **58**, 14167 (1998).
7. R. S. Iskhakov, S. V. Komogortsev, A. D. Balaev, A. V. Okotrub, A. G. Kudashov, V. L. Kuznetsov, and Yu. V. Butenko, Pis'ma Zh. Éksp. Teor. Fiz. **78** (4), 271 (2003) [JETP Lett. **78** (4), 236 (2003)].
8. S. V. Komogortsev, R. S. Iskhakov, E. A. Denisova, A. D. Balaev, V. G. Myagkov, N. V. Bulina, A. G. Kudashov, and A. V. Okotrub, Pis'ma Zh. Tekh. Fiz. **31** (11), 12 (2005) [Tech. Phys. Lett. **31** (6), 454 (2005)].
9. V. A. Logvinenko, N. F. Yudanov, G. N. Chehova, Yu. G. Kriger, L. I. Yudanova, and N. A. Rudina, Chem. Sustainable Dev. **8**, 171 (2000).
10. L. Neel, Ann. Geophysi. (CNRS) **5**, 99 (1949).
11. N. S. Akulov, Z. Phys. **69**, 278 (1931).
12. R. S. Iskhakov, S. V. Komogortsev, A. D. Balaev, and L. A. Chekanova, Pis'ma Zh. Éksp. Teor. Fiz. **72** (6), 440 (2000) [JETP. Lett. **72** (6), 304 (2000)].
13. H. Bernas, I. A. Campbell, and R. Fruchart, J. Phys. Chem. Solids **28**, 17 (1967).
14. C. Zener, Phys. Rev. **96**, 1335 (1954).
15. P. M. Bozorth, Ferromagnetism (Van Norstrand, New York, 1951; Inostrannaya Literatura, Moscow, 1951).

Translated by G. Skrebtsov